13. Nienaber CA, Rousseau H, Eggebrecht H, Kische S, Fattori R, Rehders TC, Kundt G, Scheinert D, Czerny M, Kleinfeldt T, Zipfel B, Labrousse L, Ince H. Randomized comparison of strategies for type B aortic dissection: the INvestigation of STEnt Grafts in Aortic Dissection (INSTEAD) trial. *Circulation* 2009;120:2519–2528.
14. Kodama K, Nishigami K, Sakamoto T, Sawamura T, Hirayama T, Misumi H, Nakao K. Tight heart rate control reduces secondary adverse events in patients with type B acute aortic dissection. *Circulation* 2008;118:S167–S170.
15. Ahimastos AA, Aggarwal A, D'Orsa KM, Formosa MF, White AJ, Savarirayan R, Dart AM, Kingwell BA. Effect of perindopril on large artery stiffness and aortic root diameter in patients with Marfan syndrome: a randomized controlled trial. *JAMA* 2007;298:1539–1547.
16. Mochizuki S, Dahlöf B, Shimizu M, Ikewaki K, Yoshikawa M, Taniguchi I, Ohta M, Yamada T, Ogawa K, Kanae K, Kawai M, Seki S, Okazaki F, Taniguchi M, Yoshida S, Tajima N; Jikei Heart Study Group. Valsartan in a Japanese population with hypertension and other cardiovascular disease (Jikei Heart Study): a randomised, open-label, blinded end point morbidity-mortality study. *Lancet* 2007;369:1431–1439.
17. Sawada T, Yamada H, Dahlöf B, Matsubara H; KYOTO HEART Study Group. Effects of valsartan on morbidity and mortality in uncontrolled hypertensive patients with high cardiovascular risks: KYOTO HEART Study. *Eur Heart J* 2009;30:2461–2469.
18. Habashi JP, Judge DP, Holm TM, Cohn RD, Loeys BL, Cooper TK, Myers L, Klein EC, Liu G, Calvi C, Podowski M, Neptune ER, Halushka MK, Bedja D, Gabrielson K, Rifkin DB, Carta L, Ramirez F, Huso DL, Dietz HC. Losartan, an AT1 antagonist, prevents aortic aneurysm in a mouse model of Marfan syndrome. *Science* 2006;312:117–121.
19. Brooke BS, Habashi JP, Judge DP, Patel N, Loeys B, Dietz HC III. Angiotensin II blockade and aortic-root dilation in Marfan's syndrome. *N Engl J Med* 2008;358:2787–2795.
20. Tsai TT, Evangelista A, Nienaber CA, Myrmel T, Meinhardt G, Cooper JV, Smith DE, Suzuki T, Fattori R, Llovet A, Froehlich J, Hutchison S, Distante A, Sundt T, Beckman J, Januzzi JL Jr, Isselbacher EM, Eagle KA; International Registry of Acute Aortic Dissection. Partial thrombosis of the false lumen in patients with acute type B aortic dissection. *N Engl J Med* 2007;357:349–359.
21. Tsai TT, Fattori R, Trimarchi S, Isselbacher E, Myrmel T, Evangelista A, Hutchison S, Sechtem U, Cooper JV, Smith DE, Pape L, Froehlich J, Raghupathy A, Januzzi JL, Eagle KA, Nienaber CA; International Registry of Acute Aortic Dissection. Long-term survival in patients presenting with type B acute aortic dissection: insights from the International Registry of Acute Aortic Dissection. *Circulation* 2006;114:2226–2231.
22. Tsai TT, Evangelista A, Nienaber CA, Trimarchi S, Sechtem U, Fattori R, Myrmel T, Pape L, Cooper JV, Smith DE, Fang J, Isselbacher E, Eagle KA; International Registry of Acute Aortic Dissection (IRAD). Long-term survival in patients presenting with type A acute aortic dissection: insights from the International Registry of Acute Aortic Dissection (IRAD). *Circulation* 2006;114:I350–I356.
23. Mehta RH, Suzuki T, Hagan PG, Bossone E, Gilon D, Llovet A, Maroto LC, Cooper JV, Smith DE, Armstrong WF, Nienaber CA, Eagle KA; International Registry of Acute Aortic Dissection (IRAD) Investigators. Predicting death in patients with acute type A aortic dissection. *Circulation* 2002;105:200–206.
24. Suzuki T, Mehta RH, Ince H, Nagai R, Sakomura Y, Weber F, Sumiyoshi T, Bossone E, Trimarchi S, Cooper JV, Smith DE, Isselbacher EM, Eagle KA, Nienaber CA; International Registry of Aortic Dissection. Clinical profiles and outcomes of acute type B aortic dissection in the current era: lessons from the International Registry of Aortic Dissection (IRAD). *Circulation* 2003;108:II312–II317.
25. Sakakura K, Kubo N, Ako J, Fujiwara N, Funayama H, Ikeda N, Nakamura T, Sugawara Y, Yasu T, Kawakami M, Momomura S. Determinants of long-term mortality in patients with type B acute aortic dissection. *Am J Hypertens* 2009;22:371–377.

Hybrid repair of a Kommerell diverticulum associated with a right aortic arch and a left descending aorta

Hiroyuki Kawajiri, MD, Hideyuki Shimizu, MD, PhD, Akihiro Yoshitake, MD, PhD, and **Ryohei Yozu, MD, PhD,** *Tokyo, Japan*

This report describes the first successful case of a hybrid endovascular approach for management of aneurysmal Kommerell diverticulum arising from the left descending aorta in a right aortic arch. This patient also had dilatation of the ascending aorta and a small aortic arch aneurysm. This three-step procedure consisted of (1) ascending aorta replacement with total debranching using a handmade quarto-branched composite graft; (2) endovascular exclusion of Kommerell diverticulum and the aortic arch aneurysm by covering the whole aortic arch; and (3) coil embolization against the root of the left subclavian artery. The patient had no complications at 16 months after completion. (J Vasc Surg 2012;56:1727-30.)

A right aortic arch connected to a left descending aorta is a rare congenital defect, and Kommerell diverticulum is an aneurysm arising from an aberrant subclavian artery from the descending aorta. Although there are many reports that describe the treatment of Kommerell diverticulum arising from a right descending aorta in a right aortic arch, there are no reports that describe management of a Kommerell diverticulum arising from a left descending aorta in a right aortic arch.

Surgery via thoracotomy or a median sternotomy approach has usually been used to treat this aneurysm but can result in significant surgical mortality.[1,2] In the case of a right aortic arch connected to a left descending aorta, a surgical approach is even more challenging because of the trachea overriding the aortic arch.

Recently, a hybrid endovascular treatment for Kommerell diverticulum has been described.[3-9] The present report describes the first successful case of a hybrid endovascular treatment for aneurysmal Kommerell diverticulum arising from a left descending aorta in a right aortic arch.

CASE REPORT

A 67-year-old man was diagnosed with a 6.5-cm aneurysmal Kommerell diverticulum from a left descending aorta in a right aortic arch. This finding was in association with ascending aortic dilatation (5.0 cm in diameter) and a small aortic arch aneurysm (Fig 1, *A* and *B*). The patient's history was notable for multiple sternotomies. His first sternotomy was performed 25 years ago for back pain and a diagnosis of an aortic arch dissection. However, the surgery was not completed because the dissection was localized in the transverse arch aorta and because of complicated anatomy. The precise details of this operation were not available because the records were not fully preserved. A second sternotomy for false-lumen entry closure was performed for the dissected aortic aneurysm in the transverse arch aorta 17 years before the current presentation. In this operation, the right subclavian artery was ligated at its root because it had dissected and was too fragile to reconstruct. The blood flow of the right subclavian artery was preserved via collateral flow from the vertebral-basilar system.

The anatomy was complicated, and tight adhesion was expected. To avoid high-risk total arch replacement, the patient was offered a less invasive, three-staged hybrid endovascular procedure.

First, ascending aorta replacement and aortic arch debranching were performed with cardiopulmonary bypass established from the femoral artery to the right atrium and via selective antegrade cerebral perfusion through the distal bilateral carotid arteries. Hypothermic systemic circulatory arrest with antegrade cerebral perfusion was applied for the open distal anastomosis of the ascending aorta replacement with insertion of an elephant trunk graft into the aortic arch to establish an appropriate proximal landing zone for the next endovascular step. The systemic circulatory arrest was performed for 39 minutes at 26°C. A handmade quarto-branched composite graft, composed of a 30-mm Intervascular graft (MAQUET GmbH & Co KG, Rastatt, Germany) attached to a 16- × 8- × 7-mm InterGard Quattro graft (MAQUET GmbH & Co KG) was used (Fig 2, *A*). The bilateral carotid arteries and subclavian arteries were reconstructed using a quatro-branch. Because there was tight adhesion around the aortic arch and it was difficult to dissect its trunks, they were reconstructed through a distal approach. Arteries were anastomosed to each graft in an end-to-end fashion. However, the left subclavian artery was anastomosed in an end-to-side fashion to serve as an access for subsequent coil embolization of the root of the left subclavian artery, which was necessary to stop the blood supply to the aneurysm from the left vertebral artery (Fig 3, *A* and *B*). Coil embolization was chosen instead of ligating the left subclavian artery prox-

From the Department of Cardiovascular Surgery, Keio University School of Medicine.

Author conflict of interest: none.

Reprint requests: Hiroyuki Kawajiri, MD, Department of Cardiovascular Surgery, Keio University School of Medicine, 35 Shinanomachi, Shinjuku, Tokyo 160-8582, Japan (e-mail: hiroyukikawajiri607023@gmail.com).

The editors and reviewers of this article have no relevant financial relationships to disclose per the JVS policy that requires reviewers to decline review of any manuscript for which they may have a conflict of interest.

0741-5214/$36.00

http://dx.doi.org/10.1016/j.jvs.2012.05.093

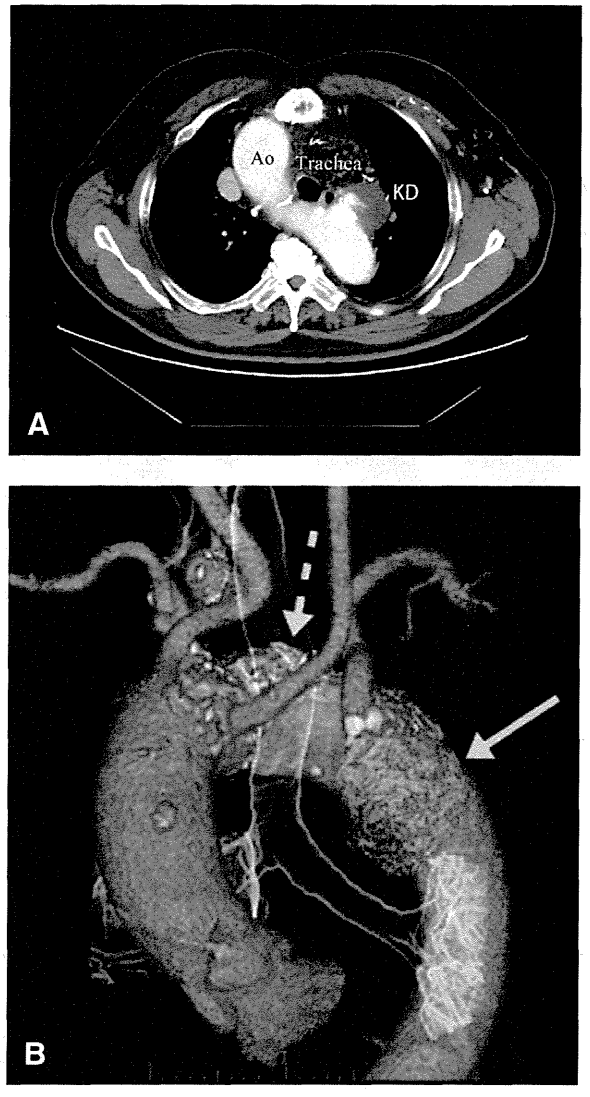

Fig 1. A, Preoperative computed tomography scan shows the right aortic arch (*Ao*) connected to the left descending aorta. The trachea overrides the aortic arch. *KD,* Kommerell diverticulum. **B,** Two aneurysms are shown as blue-colored areas: a 6.5-cm aneurysmal Kommerell diverticulum (*solid arrow*), and a 4.0-cm saccular-type aneurysm (*dotted arrow;* not enhanced because of thromboembolism).

imal to the left vertebral artery, because this approach was considered to be easier and safer with lower risk of coil migration in the context of insertion of an endovascular graft into the aortic arch. After this procedure, the patient developed pneumonia and had difficulty swallowing, but was discharged on postoperative day 56 with full recovery.

Three months after the operation, the patient was admitted to the hospital for planned endovascular aneurysm exclusion through a femoral access. A Talent endovascular graft (Talent TF3434; Medtronic, Minneapolis, Minn) was inserted into the elephant trunk 1 cm distal to the prior distal anastomosis, followed by a second Talent graft (Talent TF4040) that had been fitted to land on the distal aortic

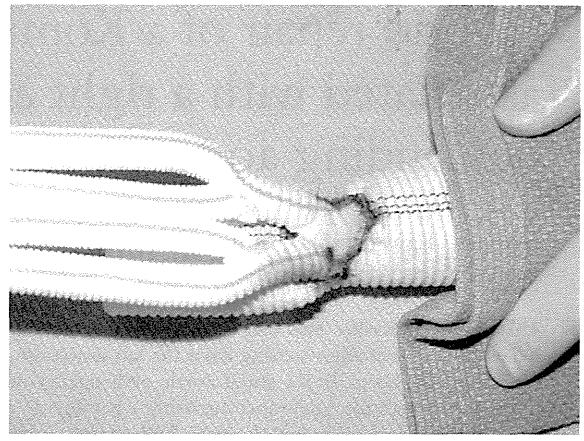

Fig 2. Handmade quarto-branched composite graft.

arch with an overlap of two stents between the endografts. Complete aortic arch covering was achieved with covering arch trunks (Fig 3, *C*). Ten days later, coil embolization was performed for the root of the left subclavian artery through left brachial access. The patient had no postoperative complications and was discharged 2 days after coil embolization. He remained asymptomatic without any complications over the 12-month follow-up period.

DISCUSSION

Kommerell first described an aberrant right subclavian artery originating from the descending thoracic aorta of a left aortic arch that was associated with persistence of a remnant of the right dorsa aorta.[10] In a review of the literature regarding Kommerell aneurysms, Austin et al[1] reported that 19% of patients presented with rupture and death. In a review of the literature of Kommerell diverticulum associated with the right aortic arch reported by Cinà et al,[2] 53% of the 32 cases presented with rupture or dissection.

A right aortic arch connected to a left descending aorta with an aberrant left subclavian artery is extremely rare, but several cases have been reported.[11] However, there are no case reports that describe treatment for Kommerell diverticulum from a left descending aorta in a right aortic arch.

An aortic arch replacement via thoracotomy or a median sternotomy approach has been conventionally applied for an aneurysmal Kommerell diverticulum to prevent its rupture or dissection. However, this surgical treatment is associated with a high mortality rate ranging from 12%[2] to 16.6%.[1,2] In the case of a right aortic arch connected to a left descending aorta, the trachea overrides the aortic arch and the estimated surgical risk is extremely high.

A hybrid endovascular treatment for aneurysmal Kommerell diverticulum has recently been described.[3-9] Frigatti et al[9] conducted a hybrid two-step procedure, consisting of a total aortic debranching and endovascular aneurysm exclusion.

In the present case, two difficulties were considered with regard to the endovascular approach. First, a small

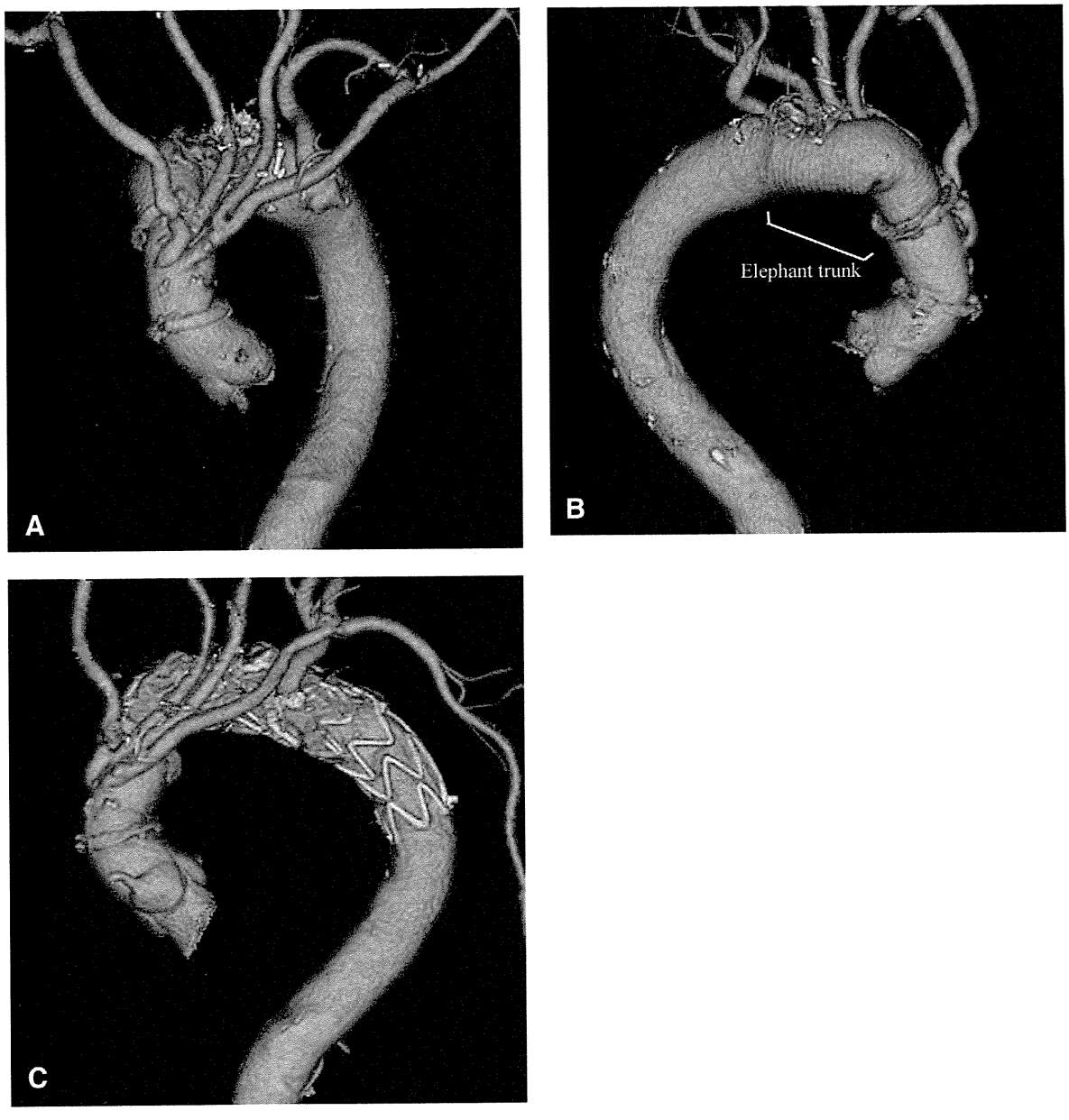

Fig 3. A, Front view of postoperative computed tomography scan. **B,** Back view shows a long insertion of an elephant trunk graft. **C,** Postendovascular treatment computed tomography scan shows complete covering of the aortic arch with the endovascular graft.

aortic arch aneurysm was located between the left carotid artery and the left subclavian artery. To cover this small aneurysm and to establish an extended landing zone proximal to the carotid arteries, total debranching was needed. Second, the aneurysmal portion of the ascending aorta was about 5.0 cm in diameter, making it unlikely that we could obtain a good fit using any commercially available endografts. Therefore, ascending aorta replacement was performed using a handmade quatro-branched composite graft to make an appropriate proximal landing zone before endovascular treatment was conducted.

CONCLUSIONS

This report describes a case in which the extended hybrid approach, consisting of ascending aorta replacement, total debranching, and endovascular treatment, was successfully used to treat an aneurysmal Kommerell diverticulum arising from a left descending aorta in a right aortic arch associated with ascending aorta dilatation and an

aortic arch aneurysm. Use of this hybrid endovascular approach may help reduce complications and mortality in complex and challenging aortic cases.

REFERENCES

1. Austin EH, Wolfe WG. Aneurysm of aberrant subclavian artery with a review of the literature. J Vasc Surg 1985;2:571-7.
2. Cinà CS, Althani H, Pasenau J. Abouzahr L. Kommerell's diverticulum and right-sided aortic arch: A cohort study and review of the literature J Vasc Surg 2004;39:131-9.
3. Davidian M, Kee ST, Kato N, Semba CP, Razavi MK, Mitchell RS, et al. Aneurysm of an aberrant right subclavian artery: Treatment with PTFE covered stentgraft. J Vasc Surg 1998;28:335-9.
4. Corral JS, Zúñiga CG, Sánchez JB, Guaita JO, Basail AM, Gimeno CC. Treatment of aberrant right subclavian artery aneurysm with endovascular exclusion and adjunctive surgical bypass. J Vasc Interv Radiol 2003;14:789-92.
5. Lacroix V, Astarci P, Philippe D, Goffette P, Hammer F, Verhelst R, et al. Endovascular treatment of an aneurysmal aberrant right subclavian artery. J Endovasc Ther 2003;10:190-4.
6. Attmann T, Brandt M, Müller-Hülsbeck S, Cremer J. Two-stage surgical and endovascular treatment of an aneurysmal aberrant right subclavian (Lusoria) artery. Eur J Cardiothorac Surg 2005; 27:1125-7.
7. Kopp R, Wizgall I, Kreuzer E, Meimarakis G, Weidenhagen R, Kühnl A, et al. Surgical and endovascular treatment of symptomatic aberrant right subclavian artery (arteria lusoria). Vascular 2007;15: 84-91.
8. Shennib H, Diethrich EB. Novel approaches for the treatment of the aberrant right subclavian artery and its aneurysms. J Vasc Surg 2008; 47:1066-70.
9. Frigatti P, Grego F, Deriu GP, Lepidi S. Hybrid endovascular treatment of aneurysm degeneration in a rare right-aortic arch anomaly with Kommerell diverticulum. J Vasc Surg 2009;50:903-6.
10. Kommerell B. Relocation of the esophagus by an abnormal subclavian artery runs artery (arteria lusoria) [Article in German]. Fortschr Geb Roentgenstr 1936;54:590-5.
11. Barcudi S, Sanders SP, Di Donato RM, de Zorzi A, Iacobelli R, Amodeo A, et al. Aberrant left innominate artery from the left descending aorta in right aortic arch: Echocardiographic diagnosis. J Am Soc Echocardiogr 2010;23:221.e5-221.e7.

Submitted Mar 23, 2012; accepted May 27, 2012.

Combined use of an epidural cooling catheter and systemic moderate hypothermia enhances spinal cord protection against ischemic injury in rabbits

Shinya Inoue, MD,[a] Atsuo Mori, MD,[b] Hideyuki Shimizu, MD,[a] Akihiro Yoshitake, MD,[a] Ryoichi Tashiro, PhD,[b] Nobuyuki Kabei, PhD,[b] and Ryohei Yozu, MD[a]

Background: Epidural placement of a cooling catheter can protect against ischemic spinal cord injury. With the use of rabbits, we investigated whether this epidural cooling technique, when combined with systemic moderate hypothermia, can protect the spinal cord against ischemic metabolic stress.

Methods: New Zealand white rabbits (n = 28) were assigned to 1 of 4 different groups. Animals underwent abdominal aortic occlusion for 30 minutes using a 3F balloon catheter. Group 1 (n = 7) underwent epidural cooling by the catheter and systemic moderate hypothermia (35°C) induced with a cooling blanket. Group 2 (n = 7) underwent epidural cooling under systemic normothermia (38.5°C). Group 3 (n = 7) underwent systemic moderate hypothermia (35°C) without epidural cooling. Group 4 (n = 7) underwent neither epidural nor blanket cooling as a negative control. Neurologic status of their hind limbs was graded according to the modified Tarlov scale at 1, 2, and 7 days after surgery.

Results: During infrarenal aortic ischemia, epidural temperature was significantly lower in group 1 (18.5°C ± 0.8°C) than in group 2 (28.6°C ± 1.0°C; $P = .0001$), group 3 (34.2°C ± 0.06°C; $P = .0001$), or group 4 (38.5°C ± 0.2°C; $P = .0001$). Hind limb function recovery was greater in group 1 (mean Tarlov score, 4.9 ± 0.057) than in group 2 (2.6 ± 0.3; $P = .0028$), group 3 (2.1 ± 0.34; $P = .0088$), or group 4 (0.0 ± 0.0; $P = .0003$).

Conclusions: Epidural cooling catheter combined with systemic moderate hypothermia produced additive cooling ability and protected the spinal cord against ischemia in rabbits more effectively than either intervention alone. (J Thorac Cardiovasc Surg 2012;■:1-6)

ET/BS

Although cardiovascular surgeons have achieved a substantial reduction in the incidence of paraplegia associated with surgery for thoracic aortic aneurysm and thoracoabdominal aortic aneurysm (TAA), this dreaded complication has not been completely eliminated. Since the 1950s, hypothermia has been demonstrated to protect against ischemic spinal cord injury.[1-3] However, general body hypothermia involves various risks, including coagulopathy, arrhythmia, and respiratory dysfunction. Local spinal cord cooling was developed to avoid the detrimental effects of systemic hypothermia while preserving its protective effects. Although favorable clinical experience with regional cooling by infusing iced saline into the epidural space was reported, elevated intrathecal pressure resulting from the infused saline presented a major concern.[4,5]

To overcome the problem of local cooling via infusion of cold saline into the epidural space, we developed a novel epidural cooling technique using a U-looped catheter containing circulating iced saline in its closed lumen. In an experimental study in pigs, the cold epidural catheter protected the spinal cord against paraplegia without elevating intrathecal pressure.[6] Since the original design, we have incorporated a counter current lumen within the epidural cooling catheter, which permits percutaneous installation. This revised system also was protective against ischemic spinal cord injury.[7] We have further refined the system by reducing the catheter diameter to facilitate clinical use.[8]

Systemic moderate hypothermia (32°C-34°C) induced by partial extracorporeal bypass is used in the clinical setting to protect the spinal cord during aortic surgery.[6] The goal of this study was to determine whether combined use of our epidural cooling technique and systemic moderate hypothermia may cool the spinal cord more effectively and whether this combination results in better protection against ischemic spinal cord injury.

MATERIAL AND METHODS

Continuous Cord Cooling System and Epidural Cooling Catheter

The basic concept of our cooling catheter has been described in a previous study.[6] The cooling system is composed of 3 units: a saline-filled

From the Department of Cardiovascular Surgery,[a] Keio University School of Medicine, Shinjuku, Tokyo, Japan; and Department of Cardiovascular Surgery,[b] Saitama Cardiovascular and Respiratory Center, Kumagaya, Saitama, Japan.

Disclosures: Authors have nothing to disclose with regard to commercial support.
Received for publication Oct 5, 2012; revisions received Nov 6, 2012; accepted for publication Nov 12, 2012.

Address for reprints: Shinya Inoue, MD, Department of Cardiovascular Surgery, Keio University School of Medicine, 35 Shinanomachi, Shinjuku-ku, Tokyo, Japan 1608582 (E-mail: inoueshinya1972@yahoo.co.jp).

0022-5223/$36.00

http://dx.doi.org/10.1016/j.jtcvs.2012.11.040

Abbreviation and Acronym
TAA = thoracoabdominal aortic aneurysm

cooling catheter in the epidural space, an external cooling unit, and an external circulating pump. In the current study, saline was cooled by the outer cooling unit to 4°C and circulated at a rate of 40 mL/min by an external pump (AST Co, Ltd, Higashimatsuyama, Japan).

The polyurethane cooling catheter (Unitika, Tokyo, Japan), in which iced saline could circulate without leakage, was 15 cm in length and had an 18-gauge outer diameter (Figure 1). A smaller-diameter catheter (18-gauge) was designed for use in rabbits. The coolant entered the inlet limb of the cooling catheter, passed through the lumen to the tip of it, and returned back to the outlet limb. The fluid is not able to leak out of the inner lumen to the epidural space.

Animal Model, Surgical Procedure, and Cooling Protocol

A total of 28 New Zealand white rabbits (weighing 3.0-3.5 kg) were used. Animals were randomly assigned to 1 of 4 different groups: a regional cooling by epidural catheter combined with systemic moderate hypothermia (35°C) by cooling blanket (group 1), a regional cooling by epidural catheter under systemic normothermia (38.5°C) (group 2), systemic moderate hypothermia (35°C) by cooling blanket without epidural cooling (group 3), and a negative control group without regional cooling under systemic normothermia (group 4).

Rabbits were initially anesthetized with 1.5% isoflurane added to a mixture of 30% oxygen and 68.5% air. Animals underwent endotracheal intubation and breathed spontaneously without mechanical ventilation. Electrocardiogram, arterial pressure, and rectal temperature were monitored continuously.

First, rabbits were placed in the prone position. A dorsal midline skin incision, 5 cm in length, was made at the levels of Th12 and L1. The spinous process and intervertebral ligament were excised to expose the ligamentum flavum, which was incised between Th12 and L1 to create a small defect for entry into the epidural space. An epidural cooling catheter was then introduced at that site and advanced into the epidural space. It was directed caudally along the midline of the space to the L7 level, followed by connection to the external unit. A thermistor probe was placed on the dorsal dural surface at the level of L1 to record the epidural temperature (Figure 2, *A* and *B*).

Next, with the rabbit in the supine position, the right femoral artery was dissected. In all groups, animals underwent 30 minutes of infrarenal aortic ischemia via balloon occlusion. Heparin sulfate (50 U/kg) was administered as an intravenous bolus. A Fogarty balloon catheter (3F) was introduced from the right femoral artery into the abdominal aorta. Under fluoroscopic guidance, the balloon of the catheter was placed immediately below the renal arteries. In rabbits, arteries that feed the spinal cord arise from the abdominal aorta. Therefore, the inflation of the balloon at this position results in abdominal aortic occlusion and spinal cord ischemia.

A cooling/warming blanket was used to control systemic temperature. In groups 1 and 3, the animals were cooled to 35°C (rectal temperature) by a cooling blanket. In groups 2 and 4, a cooling/warming blanket was used to maintain normal body temperature (38.5°C). In groups 1 and 2, animals underwent local cooling with the epidural catheter 30 minutes before balloon occlusion. During the 30 minutes of balloon occlusion, epidural cooling was continued via the catheter. After deflation of the balloon, epidural cooling was continued for 30 minutes to slow the increase of spinal temperature accompanying reperfusion. In groups 3 and 4, the epidural catheter was placed in the same fashion as in groups 1 and 2, but the rabbits did not undergo epidural cooling at any point during the procedure.

After surgery, the epidural catheter, the Fogarty balloon catheter, and all measuring probes were removed, and the wounds in the back and groin were closed. The animals were extubated and returned to cages with free access to water and food. They received humane care and treatment in accordance with the "Guide for the Care and Use of Laboratory Animals" (www.nap.edu/catalog/5140.html). Further, the experimental and animal care protocols were approved by the Animal Care Committee of the Saitama Cardiovascular and Respiratory Center, Saitama, Japan.

Neurologic Evaluation

Neurologic status with respect to hind limb function was assessed at 1, 2, and 7 days after the operation according to a modified Tarlov scale: 0 = no movement, 1 = slight movement, 2 = sits with assistance, 3 = sits alone, 4 = weak hop, 5 = normal hop.

Histologic Examination

On the seventh day after surgery, animals were reanesthetized and killed with an intravenous overdose of pentobarbital. After perfusion fixation with 4% phosphate-buffered paraformaldehyde, the spinal cords were removed rapidly. This was followed by immersion fixation in the same solution for 2 weeks. Cross-sections of the spinal cord were stained with hematoxylin–eosin. Histologic assessment was performed using light microscopy.

For quantitative histopathologic analysis, the spinal cord was divided into the 4 lumbar segments. Twenty-eight specimens in each group were reviewed by a pathologist who was blinded to the experimental group. Motor neurons with normal appearance were counted in each segment.

Statistical Analysis

The Mann–Whitney *U* test was used to compare the postoperative neurologic status between any 2 groups of animals, and the Student *t* test was used to compare the number of motor neurons. Analysis of variance for repeated measures was carried out on variables assessed at multiple times.

RESULTS

Temperature

Epidural temperatures of the 4 groups are shown in Figure 3.

In group 1, epidural temperature at 30 minutes before aortic occlusion was 38.7°C ± 0.6°C and decreased to 20.0°C ± 2.5°C by the time of aortic occlusion ($P < .0001$). At the termination of aortic occlusion, epidural temperature had decreased further to 17.9°C ± 2.2°C. Baseline rectal temperature (38.9°C ± 0.2°C) had decreased significantly to 35.2°C ± 0.2°C by the time of aortic occlusion ($P < .0001$). A significant difference was evident between epidural (17.6°C ± 2.2°C) and rectal (35.0°C ± 0.2°C) temperatures at the termination of aortic occlusion in group 1 ($P < .0001$).

During the aortic interruption, epidural temperature was significantly lower in group 1 (18.5°C ± 0.8°C) than in group 2 (28.6°C ± 1.0°C; $P < .0001$), group 3 (34.2°C ± 0.06°C; $P < .0001$), or group 4 (38.5°C ± 0.2°C; $P < .0001$). Epidural temperature during aortic occlusion was significantly lower in group 2 than in group 4 ($P < .0001$), significantly lower in group 3 than in group 4 ($P < .0001$), and significantly lower in group 2 than in group 3 ($P < .0001$).

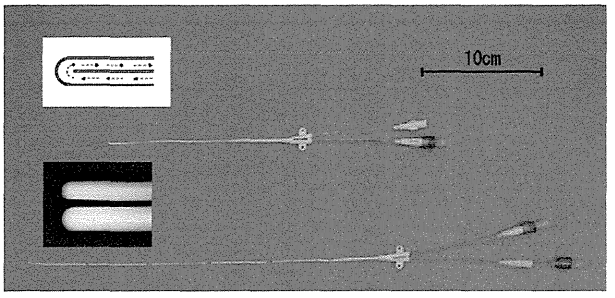

FIGURE 1. Epidural cooling catheter with a smaller lumen (18-gauge) compared with the former one we used in pigs. Cold saline circulates in a closed lumen without epidural leakage.

In group 1, epidural temperature at 30 minutes after reperfusion of group 1 (27.7°C ± 3.2°C) was significantly higher than at termination of aortic occlusion (17.9°C ± 2.2°C) ($P < .0001$). Further, in group 2, epidural temperature after reperfusion (33.1°C ± 1.5°C) was significantly higher than that at the time of balloon deflation (27.4°C ± 1.5°C) ($P < .0001$).

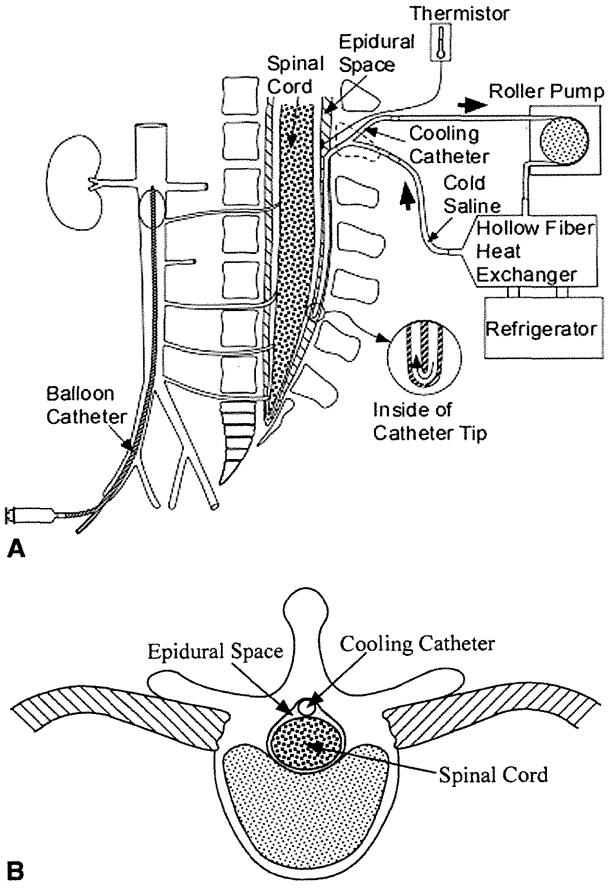

FIGURE 2. A, Schematic illustration of continuous cord cooling system in the experimental setting. A cooling catheter was introduced into the epidural space caudally. A Fogarty balloon (3F) was inserted into the abdominal aorta to induce spinal cord ischemia. B, A cooling catheter was placed in the epidural space to cool the spinal cord.

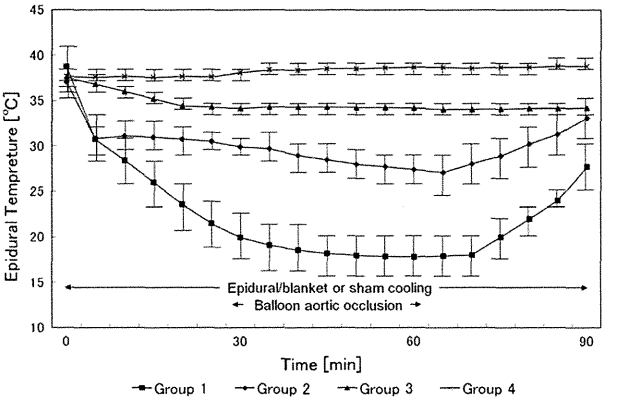

FIGURE 3. Changes in epidural temperatures during the procedure in the 4 animal groups. *Filled squares, filled diamonds, filled triangles,* and *crosses* represent groups 1, 2, 3, and 4, respectively.

Epidural temperature during reperfusion was significantly lower in group 1 (21.1°C ± 3.7°C) than in group 2 (29.4°C ± 2.2°C; $P = .00013$) or group 3 (34.1°C ± 0.1°C; $P < .0001$).

Rectal temperatures at the time of aortic occlusion were significantly lower in group 1 (35.2°C ± 0.2°C) and group 3 (35.5°C ± 0.2°C) than in group 2 (38.5°C ± 0.9°C) and group 4 (39.5°C ± 0.2°C) (Figure 4).

Recovery of Motor Function

Neurologic outcomes by scoring hind limb function are shown in Table 1.

All rabbits in group 4 exhibited complete paraplegia on the seventh day after surgery. By contrast, group 1 animals recovered fully. Functional recovery was better in group 1 (mean Tarlov score, 4.9 ± 0.057) than in group 2 (2.6 ± 0.3; $P = .0028$), group 3 (2.1 ± 0.34; $P = .0088$),

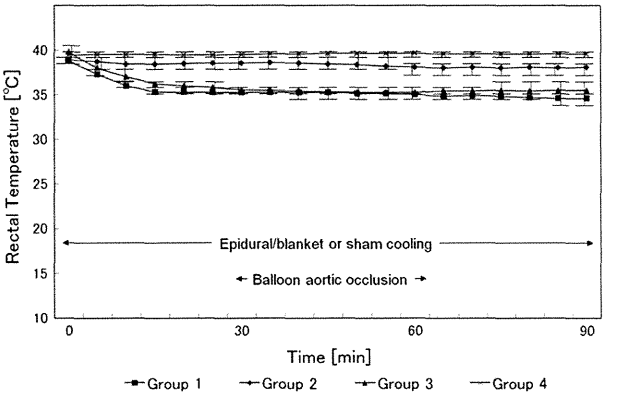

FIGURE 4. Changes in rectal temperatures during the procedure in the 4 animal groups. *Filled squares, filled diamonds, filled triangles,* and *crosses* represent groups 1, 2, 3, and 4, respectively.

ET/BS

TABLE 1. Neurologic outcomes

Modified Tarlov scale	Group 1 (n = 7) catheter + blanket cooling			Group 2 (n = 7) catheter cooling			Group 3 (n = 7) blanket cooling			Group 4 (n = 7) control		
Scale	1 d	2 d	7 d	1 d	2 d	7 d	1 d	2 d	7 d	1 d	2 d	7 d
5	6	6	6	1	1	1	2	2	2	0	0	0
4	1	1	1	4	3	3	1	1	1	0	0	0
3	0	0	0	2	1	0	2	1	0	0	0	0
2	0	0	0	0	0	0	0	0	0	0	0	0
1	0	0	0	0	0	1	0	0	1	0	0	0
0	0	0	0	0	2	2	2	3	3	7	7	7

Hind limb function in rabbits was evaluated according to a modified Tarlov scale at 1, 2, and 7 days after surgery. Data represent numbers of animals with specified scores. Group 1 (catheter and blanket cooling) exhibited better hind limb function recovery when compared with group 2 (catheter cooling), group 3 (blanket cooling), and group 4 (control) ($P = .0028$, $P = .0088$, $P = .0003$, respectively).

or group 4 (0.0 ± 0.0; $P = .0003$). Further, functional recovery was better in group 2 and group 3 than in group 4 ($P = .0088$ and $P = .025$, respectively). There was no significant difference in the functional score on the seventh day when comparing group 2 and group 3 ($P = .84$).

Histologic Examination

Representative histologic sections from lumbar segments of the cords are shown in Figure 5.

Group 1 had normal histologic characteristics. Group 2 showed a mild neuronal change with hyperchromatic nuclei

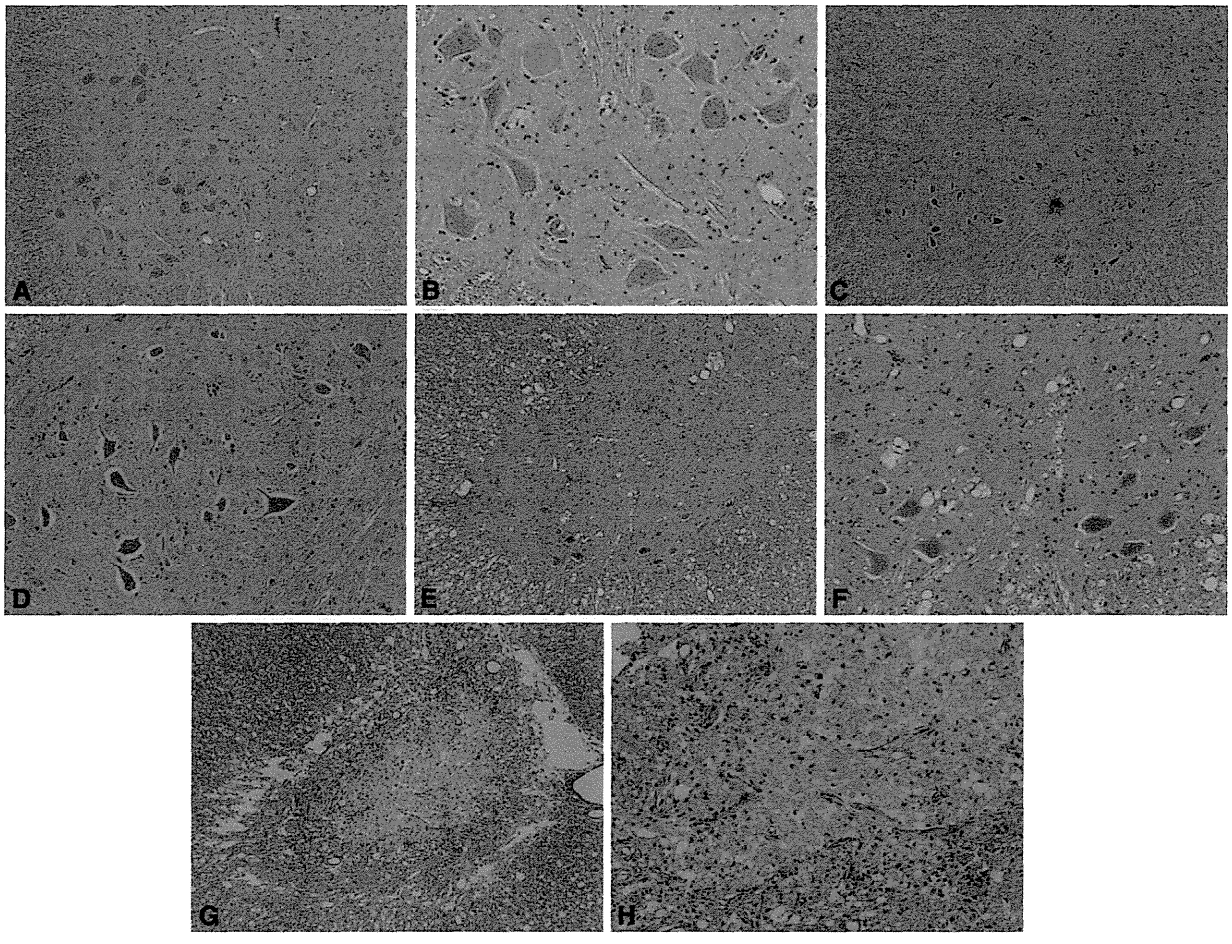

FIGURE 5. Representative photomicrographs of histologic sections of spinal cords from rabbits. A, Group 1 stained with hematoxylin–eosin (×40). B, Group 1 stained with hematoxylin–eosin (×100). C, Group 2 stained with hematoxylin–eosin (×40). D, Group 2 stained with hematoxylin–eosin (×100). E, Group 3 stained with hematoxylin–eosin (×40). F, Group 3 stained with hematoxylin–eosin (×100). G, Group 4 stained with hematoxylin–eosin (×40). H, Group 4 stained with hematoxylin–eosin (×100).

and shrunken cytoplasm in the anterior horns. There was no white matter degeneration in group 2. Group 3 exhibited moderate gray matter degeneration with motor neuron loss and mild glial proliferation. Group 4 exhibited complete loss of motor neurons with vascular necrosis. Infiltration of inflammatory cells was seen in the gray matter. Axonal vacuolization was also noted in the white matter in group 4.

No axonal injury, which would suggest a compression effect due to the epidural catheter, was observed in the dorsal portion of the spinal cord in any of the animal groups.

Figure 6 illustrates the number of motor neurons from L2 to L5 in the 4 animal groups. A greater number of large motor neurons could be seen in the gray matter of all segments in group 1 when compared with that in the corresponding segments in groups 2, 3, or 4. The mean number of motor neurons was significantly greater in group 1 (25.6 ± 1.5) than in group 2 (15.6 ± 1.9; $P = .0032$), group 3 (15.0 ± 1.8; $P = .0013$), or group 4 (3.8 ± 0.9; $P < .0001$). There was no significant difference in the number of motor neurons in all segments when comparing group 2 and group 3. The number of motor neurons was greater in group 2 and group 3 than in identical segments in group 4 ($P = .0003$ and $P = .0003$, respectively).

DISCUSSION

The present study demonstrated that the addition of topical cooling with an epidural catheter to general moderate hypothermia could further decrease the epidural temperature of the spinal cord. Further, the combination of topical and systemic hypothermia led to significantly better neurologic recovery in hind limbs after ischemic stress when compared with either modality alone or when compared with neither modality. These findings were corroborated by histologic parameters.

The rabbit model involving infrarenal aortic clamping is well established as a model of paraplegia after spinal cord ischemia.[9] The radicular arteries feed the spinal cord at the approximate level of the diaphragms in humans and pigs and at the level of abdominal infrarenal lumbar arteries in rabbits. Thus, in rabbits, infrarenal aortic occlusion for 20 minutes can induce complete paraplegia under normothermia. The present study demonstrated the synergistic action of local epidural cooling and systemic moderate hypothermia in terms of protecting the protect spinal cord for a 30-minute course of ischemic stress synergistically in rabbits.

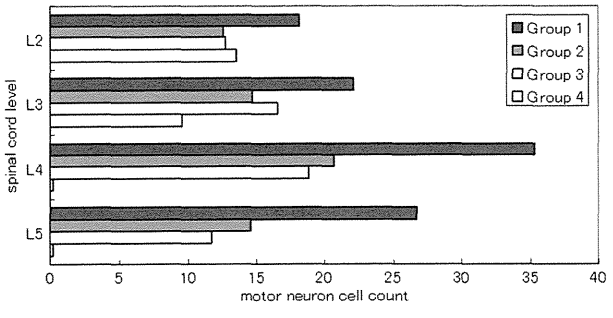

FIGURE 6. Bars represent motor neuron number from each section of excised spinal cords from L2 to L5 in the 4 animal groups.

Cambria and co-workers[4] reported that epidural cooling, via infusion of iced saline into the epidural space, could protect against paraplegia/paraparesis induced by surgical management of TAA. However, their method can increase intrathecal pressure, which itself can damage the spinal cord. To avoid an increase in intrathecal pressure, we developed a novel cooling method that uses a catheter with a closed lumen containing circulating iced saline,[6] and experiments demonstrated that this system could protect against spinal cord ischemia.

Systemic moderate hypothermia (32°C-34°C), induced by a left atrium–femoral artery shunt or a femoral vein–femoral artery partial bypass, is used for aortic surgery.[3] Therefore, the present study addressed the question of whether the combined use of epidural cooling (with our novel cooling catheter) and systemic moderate hypothermia could act in a synergistic fashion to protect against ischemic spinal cord injury.

General hypothermia is used as a basic strategy against ischemic spinal cord injury. A decrease of 5°C in body temperature decreases the metabolic rate of the spinal cord by approximately 50%. Because TAA operations are usually performed under conditions in which the heart is still beating, only moderate hypothermia (32°C-34°C) can be used.[10] Kouchoukos and colleagues[11] and Kulik and colleagues[12] reported that the incidence of paraplegia after TAA operations is low and that deep hypothermic circulatory arrest (body temperature <20°C) was effective in preventing paraplegia. However, this degree of hypothermia also can provoke some deleterious complications, including coagulopathy, arrhythmia, and respiratory dysfunction.

The present study demonstrated that decreasing the temperature of the spinal cord without lowering the systemic body temperature to deep hypothermic levels was protective against ischemic stress. We believe that the combined use of the epidural cooling catheter and moderate systemic hypothermia can be an effective method to prevent spinal cord injury in patients undergoing aortic surgery, minimizing mortality and morbidity resulting from other complications.

The spinal cord is contained within the spinal canal, and the tissues within this area (eg, bones and ligaments) produce relatively little heat. Thus, a small epidural cold catheter, assisted by the insulating effect of spinal canal, is sufficient to counteract the heat conducted from the surrounding muscles. Therefore, an epidural cooling catheter can further reduce the spinal temperature, even under the condition of systemic moderate hypothermia, leading to more protection of the spinal cord.

ET/BS

Further, from the standpoint of thermal kinetics, there is a dynamic thermal equilibrium among the spinal blood flow, spinal cord, and cooling catheter. When epidural cooling is performed, spinal blood flow provides heat to the spinal cord, whereas the catheter removes heat from the spinal cord. There was significant elevation of epidural temperature during the reperfusion phase in group 1 despite the ongoing presence of the epidural cooling catheter. We speculate that balloon deflation resulted in an increase in spinal cord blood flow, providing more heat to the ischemic segment of the cord.

In a previous study using pigs, we reported that spinal cord tissue blood flow transiently increased up to 113% and then decreased by 32% versus baseline during reperfusion.[13] We believe that prevention of reactive hyperemia and delayed hypoperfusion was an important mechanism mediating hypothermia-induced protection against ischemic spinal cord injury. The combination of local cooling and general moderate hypothermia may decrease reperfusion injury, thereby protecting the spinal cord after the release of the aortic crossclamp.

In regard to delayed paraplegia in rabbits of group 2 or 3, multiple biologic pathways, including induction of caspase3 and glutamate neurotoxicity, might provoke neuronal apoptosis or programmed death.[14,15]

The fact that we were able to place an 18-gauge cooling catheter into the epidural space of a rabbit weighing 3.0 to 3.5 kg suggests that we may be able to apply this cooling device in smaller patients, including small women and children.

CONCLUSIONS

This study demonstrated that the combined use of local epidural cooling and systemic moderate hypothermia produced a synergistic cooling effect and a synergistic protective effect on the spinal cord in rabbits. We believe that clinical use of this strategy could reduce the incidence of paraplegia/paraparesis in patients undergoing surgery for thoracic aortic aneurysm and TAA without provoking other complications.

References

1. DeBakey ME, Cooley DA, Creech O Jr. Resection of the aorta for aneurysms and occlusive disease with particular reference to use of hypothermia; analysis of 240 cases. *Trans Am Coll Cardiol.* 1955;5:153-7.
2. Svensson LG, Crawford ES. Cardiovascular and Vascular Disease of the Aorta. Philadelphia, PA: WB Saunders; 1997.
3. Coselli JS, LeMaire SA, Conklin LD, Köksoy C, Schmittling ZC. Morbidity and mortality after extent II thoracoabdominal aortic aneurysm repair. *Ann Thorac Surg.* 2002;73:1107-16.
4. Cambria RP, Davison JK, Zannetti S, L'Italian G, Atamian S. Thoracoabdominal aneurysm repair: perspectives over a decade with the clamp-and-sew technique. *Ann Surg.* 1997;226:294-305.
5. Tabayashi K, Niibori K, Konno H, Mohri H. Protection from postischemic spinal cord injury by perfusion cooling of the epidural space. *Ann Thorac Surg.* 1993; 56:494-8.
6. Mori A, Ueda T, Hachiya T, Kabei N, Okano H, Yozu R, et al. An epidural cooling catheter protects the spinal cord against ischemic injury in pigs. *Ann Thorac Surg.* 2005;80:1829-34.
7. Yoshitake A, Mori A, Shimizu H, Ueda T, Kabei N, Hachiya T, et al. Use of an epidural cooling catheter with a closed countercurrent lumen to protect against ischemic spinal cord injury in pigs. *J Thorac Cardiovasc Surg.* 2007;134:1220-6.
8. Shimizu H, Mori A, Yamada T, Ishikawa A, Okano H, Takeda J, et al. Regional spinal cord cooling using a countercurrent closed-lumen epidural catheter. *Ann Thorac Surg.* 2010;89:1312-3.
9. Pokhrel B, Hasegawa T, Izumi S, Ohmura A, Munakata H, Okita Y. Excessively high systemic blood pressure in the early phase of reperfusion exacerbates early-onset paraplegia in rabbit aortic surgery. *J Thorac Cardiovasc Surg.* 2010;140: 400-7.
10. Crawford ES, Coselli JS, Safi HJ. Partial cardiopulmonary bypass, hypothermic circulatory arrest, and posterolateral exposure for thoracic aortic aneurysm operation. *J Thorac Cardiovasc Surg.* 1987;94:824-7.
11. Kouchoukos NT, Masetti P, Rokkas CK, Murphy SF. Hypothermic cardiopulmonary bypass and circulatory arrest for operations on the descending thoracic and thoracoabdominal aorta. *Ann Thorac Surg.* 2002;74:S1885-8.
12. Kulik A, Castner CF, Kouchoukos NT. Outcomes after thoracoabdominal aortic aneurysm repair with hypothermic circulatory arrest. *J Thorac Cardiovasc Surg.* 2011;141:953-60.
13. Ishikawa A, Mori A, Kabei N, Yoshitake A, Suzuki T, Katori N, et al. Epidural cooling minimizes spinal cord injury after aortic cross-clamping through induction of nitric oxide synthase. *Anesthesiology.* 2009;111:818-25.
14. Mori A, Ueda T, Nakamichi T, Yasudo M, Yozu R, Kawada S, et al. Detrimental effects of exogenous glutamate on spinal cord neurons during brief ischemia in vivo. *Ann Thorac Surg.* 1997;63:1057-62.
15. Sakurai M, Nagata T, Abe K, Horinouchi T, Itoyama Y, Tabayashi K. Survival and death-promoting events after transient spinal cord ischemia in rabbits: induction of Akt and caspase3 in motor neurons. *J Thorac Cardiovasc Surg.* 2003;125: 370-7.

ET/BS

000 Combined use of an epidural cooling catheter and systemic moderate hypothermia enhances spinal cord protection against ischemic injury in rabbits

Shinya Inoue, MD, Atsuo Mori, MD, Hideyuki Shimizu, MD, Akihiro Yoshitake, MD, Ryoichi Tashiro, PhD, Nobuyuki Kabei, PhD, and Ryohei Yozu, MD, Tokyo and Saitama, Japan

The combined use of local epidural cooling and systemic moderate hypothermia produced a synergistic cooling effect and a synergistic protective effect on the spinal cord in rabbits. The clinical use of this strategy could reduce the incidence of paraplegia/paraparesis in patients undergoing surgery for thoracic aortic and thoracoabdominal aortic aneurysms without provoking other complications.

Neutrophil-Derived Matrix Metalloproteinase 9 Triggers Acute Aortic Dissection

Tomohiro Kurihara, MD; Ryoko Shimizu-Hirota, MD, PhD; Masayuki Shimoda, MD, PhD; Takeshi Adachi, MD, PhD; Hideyuki Shimizu, MD, PhD; Stephen J. Weiss, MD; Hiroshi Itoh, MD, PhD; Shingo Hori, MD, PhD; Naoki Aikawa, MD, PhD; Yasunori Okada, MD, PhD

Background—Acute aortic dissection (AAD) is a life-threatening vascular disease without effective pharmaceutical therapy. Matrix metalloproteinases (MMPs) are implicated in the development of chronic vascular diseases including aneurysm, but the key effectors and mechanism of action remain unknown. To define further the role of MMPs in AAD, we screened circulating MMPs in AAD patients, and then generated a novel mouse model for AAD to characterize the mechanism of action.

Methods and Results—MMP9 and angiotensin II were elevated significantly in blood samples from AAD patients than in those from the patients with nonruptured chronic aortic aneurysm or healthy volunteers. Based on the findings, we established a novel AAD model by infusing angiotensin II to immature mice that had been received a lysyl oxidase inhibitor, β-aminopropionitrile monofumarate. AAD was developed successfully in the thoracic aorta by angiotensin II administration to β-aminopropionitrile monofumarate-treated wild-type mice, with an incidence of 20%, 80%, and 100% after 6, 12, and 24 hours, respectively. Neutrophil infiltrations were observed in the intima of the thoracic aorta, and the overexpression of MMP9 in the aorta was demonstrated by reverse transcription polymerase chain reaction, gelatin zymography, and immunohistochemistry. The incidence of AAD was reduced significantly by 40% following the administration of an MMP inhibitor and was almost blocked completely in $MMP^{-/-}$ mice without any influence on neutrophil infiltration. Neutrophil depletion by injection of anti-granulocyte-differentiation antigen-1 (anti-Gr-1) antibody also significantly decreased the incidence of AAD.

Conclusions—These data suggest that AAD is initiated by neutrophils that have infiltrated the aortic intima and released MMP9 in response to angiotensin II. (***Circulation.* 2012;126:3070-3080.**)

Key Words: acute aortic dissection ■ MMP9 ■ leukocytes ■ angiotensin II

Acute aortic dissection (AAD) is a medical emergency that is associated with high mortality.[1] Although imaging by computed tomography and elective surgical repair represent an effective approach, there are neither specific biomarkers for prompt diagnosis nor alternative therapeutic strategies for treating the disease. The acute dangers associated with the active disease in humans do not lend itself to randomized, controlled trials, and the paucity of animal models complicates efforts to design detailed studies of the disease process. Thus, the underlying pathological mechanisms responsible for triggering the disease remain elusive.[2] Medial degeneration including cystic medial necrosis is a common histological finding in chronically damaged aortas associated with aging, hypertension, and aortic aneurysm,[3,4] and is widely accepted as an important risk factor for the development of AAD. However, the direct cellular and molecular mechanism that links the medial degeneration and the onset of AAD has not been elucidated. *Fibrillin1*-deficient (*Fibrillin1*$^{-/-}$) mice are often used as a model of Marfan syndrome, which display spontaneous development of cystic medial degeneration and ascending aortic aneurysm leading to spontaneous rupture or dissection, commonly emerging at 2 months to 4 months of age.[5] *Lysyl oxidase*-null mice develop aortic rupture spontaneously,[6] and administration of β-aminopropionitrile monofumarate (BAPN), a lysyl oxidase inhibitor, can induce cystic medial degeneration in rats.[7,8] These models have been used classically for aneurysm studies, and AAD is observed only by chance.[5,7,8] Therefore,

Received March 8, 2012; accepted October 22, 2012.

From the Department of Emergency and Critical Care Medicine (T.K., S.H., N.A.), Department of Internal Medicine (R.S.-H., H.I.), Division of Endocrinology, Metabolism and Nephrology, Department of Pathology (M.S., Y.O.), and Department of Surgery (H.S.), Division of Cardiovascular Surgery, School of Medicine, Keio University, Tokyo, Japan; First Department of Internal Medicine (T.A.), Division of Cardiology, National Defense Medical College, Saitama, Japan; and Life Sciences Institute (S.J.W.) University of Michigan, Ann Arbor, MI.

The online-only Data Supplement is available with this article at http://circ.ahajournals.org/lookup/suppl/10.1161/CIRCULATIONAHA.112.097097/-/DC1.

Correspondence to Ryoko Shimizu-Hirota, MD, PhD, Department of Internal Medicine, Division of Endocrinology, Metabolism and Nephrology, School of Medicine, Keio University, 35 Shinanomachi, Shinjuku-ku, Tokyo 160-0016, Japan or Yasunori Okada, MD, PhD, Department of Pathology, School of Medicine, Keio University, 35 Shinanomachi, Shinjuku-ku, Tokyo 160-0016, Japan. E-mail ryoko.shimizuhirota@gmail.com or okada@z6.keio.jp

Circulation **is available at http://circ.ahajournals.org** **DOI: 10.1161/CIRCULATIONAHA.112.097097**

they are not suitable for AAD models with regard to predicting the actual onset of the dissection, which is critical for understanding the pathogenesis of the disease.

Clinical Perspective on p 3080

Recent studies have demonstrated that matrix metalloproteinases (MMPs), including MMP1, 2, 3, and 9, are overproduced in a wide range of vascular diseases.[9,10] Among these MMPs, the importance of MMP9 has been documented in the development of chronic aortic aneurysm formation as a function of its ability to degrade extracellular matrix components directly, such as elastin.[11] The increased expression of MMP9, predominantly from macrophages, has also been implicated in acute vascular crises such as atherosclerotic plaque rupture and abdominal aortic aneurysm.[12–14] However, little or no information is available for the involvement of MMP9 in the development of AAD.

In the current study, we found significant elevation of MMP9 and angiotensin II (AngII) in human blood samples from AAD patients. Based on these findings, we established a novel mouse model of AAD by AngII infusion following sustained administration of BAPN. Upregulation of MMP9 from neutrophils was noted at the onset of the disease in this model. More important, genetic and pharmaceutical depletion of MMP9 attenuated dramatically the occurrence rate of AAD without impairing neutrophil infiltration. Furthermore, AngII per se induced neutrophil infiltration into aortic lesions, and neutrophil depletion by neutralizing antibody also attenuated AAD incidence. Taken together, our study provides the first evidence that MMP9 released from AngII-stimulated neutrophils initiates AAD in preconditioned aorta.

Methods

Human Blood and Affected Aortic Samples

Between April 2004 and August 2006, 16 patients diagnosed with AAD, 11 patients with acute myocardial infarction (AMI); 12 patients with chronic, nonruptured aortic aneurysm; and 16 healthy volunteers were registered in the study. All the AAD patients were free from connective tissue disorders such as Marfan syndrome, Ehlers-Danlos syndrome, and aortitis diagnosed according to the clinical history and physical examinations. They were composed of Stanford type A (6 patients) and type B (10 patients). The blood samples from AAD and AMI patients were collected within 1 hour after arrival in the hospital emergency room. AAD and AMI patients who arrived at the hospital 10 hours after onset of clinical symptoms were eliminated from the study. Diagnosis of AAD and AMI was confirmed by computed tomography and ECG, respectively. Affected aortic specimens were obtained at surgery from 10 nonruptured aortic aneurysms and 10 AAD patients, who underwent operation for aortic grafts. The human samples were collected in the Keio University Hospital, and signed informed consent for the usage of the samples for the experiments was obtained from all subjects. This study was approved by the ethics committee of the School of Medicine, Keio University.

Development of AAD Model in Mice

Wild-type (WT) and *MMP9*$^{-/-}$ mice on FVB background were purchased from Jackson Laboratory (Bar Harbor, ME). Three-week-old male mice were fed on a regular diet and administered BAPN (Sigma-Aldrich, St. Louis, MO) dissolved in drinking water (1 g/kg per day) for 4 weeks.[15] At 7 weeks of age, osmotic mini pumps (Alzet, Cupertino, CA) filled with 1 μg/kg per minute AngII (Sigma-Aldrich) or 1.3 μg/kg per minute norepinephrine (NE) (kindly provided by Daiichi-Sankyo Co. Ltd., Tokyo, Japan) were implanted subcutaneously as described previously,[16] and the mice were euthanized 24 hours after implantation. Blood pressure was measured using the tail-cuff method before and after implantation, and prior to sacrifice.[16] Mice were scanned by a microcomputed tomographic system (GE Healthcare, Tokyo, Japan) for imaging of aortas. Mouse aortas were enhanced by in situ infusion of the contrast agent, and the 3-dimensional images were reconstructed. For pharmacological depletion of MMP9, BAPN-fed mice were administered by gastric lavage with a broad-spectrum MMP inhibitor, ONO-4817 (300 mg/kg per day), which was kindly provided by Ono pharmaceutical Co. Ltd (Tokyo, Japan),[17–19] daily for 2 days before AngII administration until sacrifice. Dose of ONO-4817 (300 mg/kg per day) was determined according to information from previous studies on the pharmacokinetics and in vivo experiments.[17,18] For neutrophil depletion experiments, BAPN-fed mice received daily intraperitoneal injections of 200 μg anti-granulocyte-differentiation antigen-1 (anti-Gr-1) neutralizing antibody (R&D Systems, Minneapolis, MN) or control immunoglobulin G from 2 days before the AngII infusion until sacrifice.[20] The depletion of neutrophils was confirmed by Giemsa stain of peripheral blood smears. All studies in mice were approved by the Laboratory Animal Care and Use Committee of School of Medicine, Keio University.

Table. Background of Human Peripheral Blood and Aortic Samples

	Control (n=16)	Nonruptured Aneurysm (n=12)	AMI (n=11)	AAD (n=16)
Age, y	67±6	73±7	71±10	68±11
Male sex, n (%)	9 (56)	6 (50)	6 (55)	10 (63)
Average duration from onset, h	N/A	N/A	2.2	3.6
Hypertension, n (%)	9 (56)	7 (58)	8 (73)	12 (75)
Hyperlipidemia, n (%)	7 (44)	6 (50)	6 (55)	7 (44)

AMI indicates acute myocardial infarction; AAD, acute aortic dissection; and N/A, not applicable.

Additional Methods

The expanded Methods section in the online-only Data Supplement contains information on ELISA, histology and immunohistochemistry, reverse transcription polymerase chain reaction, gelatin zymography, film in situ zymography, and in situ detection of superoxide.

Statistics

Human blood sample data were analyzed with 2-sample *t*-tests, and the occurrence rate of mouse AAD was analyzed with Fisher's exact test. *P* value less than 0.05 was regarded as significant. *P* value was adjusted with Bonferroni method for pairwise comparisons in some experiments.

Results

Elevated Levels of MMP9 and AngII in Blood Samples From AAD Patients

We first screened the circulating levels of MMP1, MMP2, MMP3, MMP9, and metallopeptidase inhibitor 1 (TIMP1) in blood samples from healthy control volunteers and patients with nonruptured, chronic aortic aneurysm; AMI; or AAD. There were no significant differences in average age, ratio of men to women, or prevalence of major risk factors among these groups (Table). As shown in Figure 1, the AAD group exhibited significantly higher levels of MMP9 than the control, nonruptured aneurysm, or AMI groups, whereas the levels of MMP1, MMP2, MMP3, and TIMP1 did not differ among the groups.

AngII is one of the representative vasopressors implicated in the pathogenesis of many vascular diseases, including

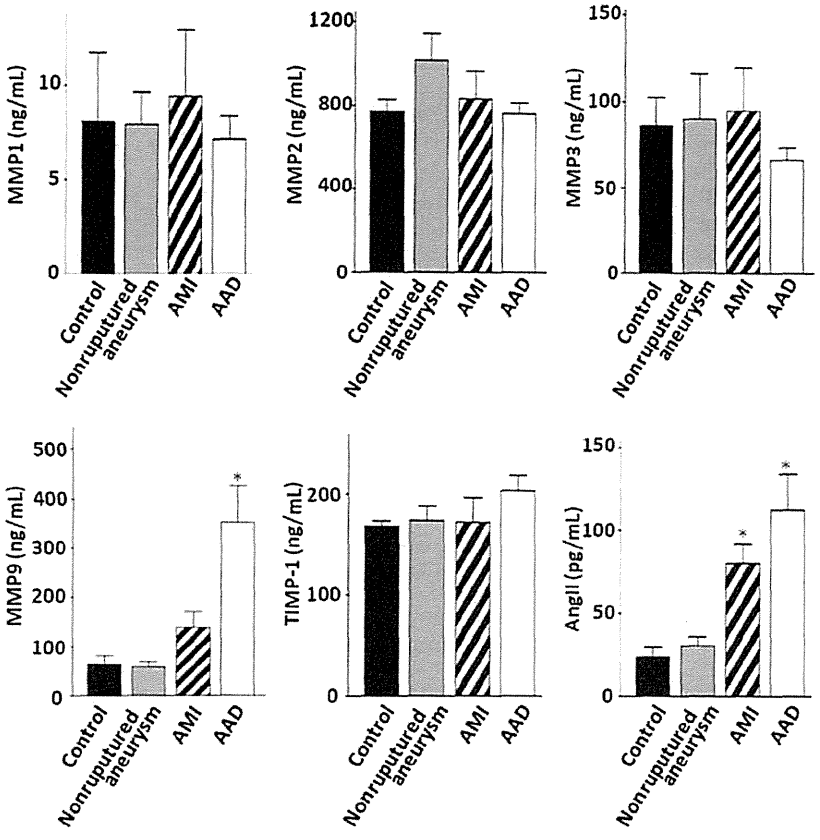

Figure 1. Circulating levels of MMP9 and AngII are elevated in the blood samples from AAD patients. MMP1, MMP2, MMP3, MMP9, TIMP-1, and AngII were assayed by the ELISA systems for each marker in the human peripheral blood samples from healthy control volunteers (n=16); patients with nonruptured, chronic aortic aneurysm (n=12); AMI (n=11); or AAD (n=16). Values are mean±SEM. The probability value was adjusted with the Bonferroni method for pairwise comparisons. *$P<0.05$ versus control. MMP9 indicates matrix metalloproteinase 9; AngII, angiotensin II; AAD, acute aortic dissection; TIMP-1, metallopeptidase inhibitor 1; and AMI, acute myocardial infarction.

aneurysm formation.[21] In addition, AngII is known to promote neutrophil infiltration into vascular walls,[22,23] and to induce MMP9 expression in cell types such as vascular smooth muscle cells.[24] Thus, we also measured the AngII levels in serum samples of the control, nonruptured aneurysm, AMI, and AAD groups, and found that the circulating AngII level was significantly higher in the AAD and AMI groups relative to the other groups studied (Figure 1).

Immunolocalization of MMP9 in Aortic Lesions From AAD Patients

Immunohistochemistry of patient samples indicated that the AAD tissues contain abundant MMP9-positive cells located mainly in the medial layer of dissected aorta, with smaller numbers of MMP9-positive cells scattered in the aortic tissues of the nonruptured aneurysm, predominantly localized to areas of the media displaying severe atherosclerotic changes (Figure 2A and 2B). Of note, neutrophils accumulated to much higher levels in the dissected aorta from the AAD patients relative to the nonruptured aneurysm (Figure 2A and 2B). Morphometric analysis of MMP9 immunoreactive cells in the aortic tissues showed a statistically significant increase in the aorta from the AAD patients (171.8±97.2 cells/mm^2) compared with that from patients with nonruptured aneurysm (47.2±40.6 cells/mm^2; $P<0.05$). Because the MMP9 staining pattern in the AAD aorta was similar to that of antineutrophil elastase (Figure 2A), these data suggested infiltrating neutrophils as the most likely source of MMP9 in the AAD aortas. Thus, we carried out double immunostaining of MMP9 and neutrophil elastase in the AAD aortic tissues and demonstrated that both proteinases colocalize in the cells (Figure 2C).

Establishment of an AAD Model by AngII Infusion to BAPN-Treated Mice

Based on the finding that both MMP9 and AngII are upregulated in human AAD, we sought to define their roles in AAD in vivo by developing a relevant mouse model. Because previous studies have shown that sustained administration of a lysyl oxidase inhibitor, BAPN, to premature rodents induces medial degeneration of aorta and results in aneurysm formation by disrupting the structural integrity of the aortic wall as a consequence of inhibiting collagen and elastin cross-linking,[7] we administered BAPN to 3-week-old WT mice for 4 weeks. Under these conditions, apparent aneurysm formation was observed secondary to the medial degeneration (Figure 3A). However, BAPN alone was not sufficient to trigger AAD (Figure 3A and 3B). Because blood pressure elevation is considered to be a major inducer of AAD,[1] we modified our protocol by infusing vasopressive-equivalent doses of AngII or NE to BAPN-treated WT mice for up to 48 hours. Blood pressure elevated equivalently from 96.3±4.6 mm Hg to 119.4±13.7 mmHg ($P<0.05$) and 111.9±5.13 mm Hg ($P<0.05$) 1 hour after the infusion of AngII or NE, respectively (data not shown). More important, 24 hours after the infusion was initiated, AngII led to AAD in all the mice examined. Furthermore, 30% of the mice died as a result of aortic rupture and subsequent hemothorax, whereas AAD was obtained in only 10% of the mice treated with NE

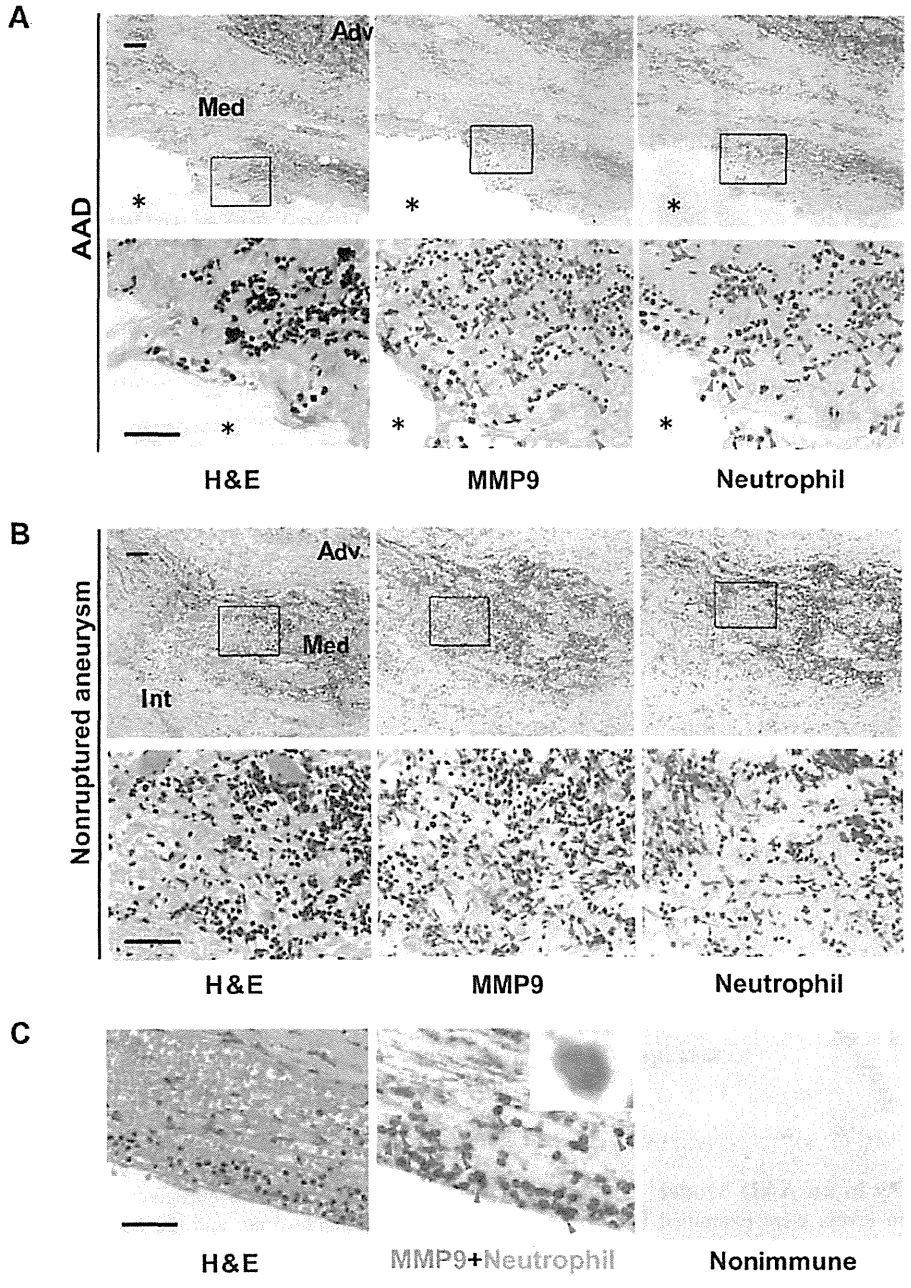

Figure 2. Dissected aortic media from AAD patients is infiltrated by numerous MMP9-positive neutrophils. Aortic tissues obtained from the patients with AAD (**A**) or nonruptured aneurysm (**B**) were subjected to histological and immunohistochemical studies for MMP9 and neutrophil elastase (Neutrophil) on serial paraffin sections. High-power view of the rectangular areas is shown in the lower rows in each panel. Asterisks indicate false lumen of the dissected aorta; red arrowheads, positively immunostained cells. Note that, in AAD samples, MMP9 is expressed by the cells mainly in the media, and the distribution of MMP9-positive cells and neutrophil elastase-positive cells is closely related. Scale bars on the upper and lower panels, 200 μm and 50 μm, respectively. **C**, Double immunostaining of MMP9 and neutrophil elastase on paraffin sections of the AAD aortic tissue. Inset shows high-power view of a double immunostained cells. Red arrowheads indicate MMP9 and neutrophil elastase-double positive cells. Scale bar, 50 μm. AAD indicates acute aortic dissection; MMP9, matrix metalloproteinase 9; Adv, adventitia; Med, media; Int, intima; H&E, hematoxylin and eosin stain; and Nonimmune, nonimmune immunoglobulin G.

infusion or BAPN treatment alone (Figure 3B). Enhanced computed tomographic scanning and histological examination demonstrated AAD in the descending thoracic aorta of the BAPN/AngII-treated mice (Figure 3A). Time course examination of AAD formation in the BAPN/AngII-treated mice demonstrated that AAD is initiated as early as 6 hours after AngII infusion, with 100% of the mice developing AAD by 24 hours (Figure 3C). Because NE infusion in BAPN-treated mice failed to induce AAD despite changes in blood pressure similar to those observed with AngII, the singular effects of AngII on triggering AAD onset are independent of blood pressure change alone.

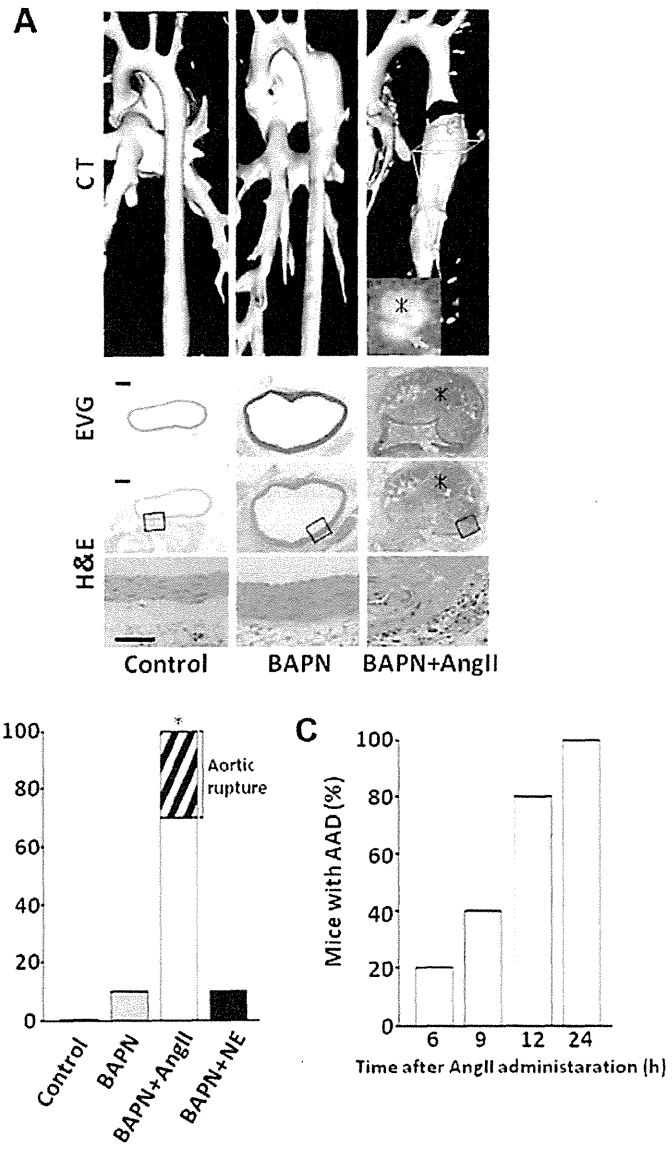

Figure 3. AngII infusion to BAPN-treated wild type (WT) mice induces AAD. **A**, Demonstration of AAD in BAPN/AngII-treated mice (BAPN+AngII) by 3-dimentional images of enhanced computed tomographic scan and histology of mouse aortas. WT mice were treated with vehicle for 4 weeks (control), BAPN alone for 4 weeks (BAPN), or BAPN for 4 weeks and then AngII for 24 hours (BAPN+AngII). The inlet in the BAPN+AngII mouse aorta (**upper**) shows the horizontal cross-section image of the dissected lesion. Arrow and asterisk indicate true and false lumens, respectively. (**Lower**) Histology of the aortas from the control, BAPN-treated, or BAPN/AngII-treated mice stained by EVG or H&E. (**Bottom**) High-power view of the rectangular areas of the middle panels. Note the aortic dissection (asterisk, false lumen) in the BAPN/AngII-treated mouse. Scale bars, 200 μm and 100 μm. **B**, AAD incidence in WT mice treated with control, BAPN alone, BAPN+AngII, or BAPN and NE (BAPN+NE) (n=10 for each group). Shaded area in BAPN/AngII-treated group denotes aortic rupture with dissection. The probability value was adjusted with the Bonferroni method for pairwise comparisons. *P<0.05 versus control. **C**, AAD incidence in BAPN-treated WT mice at different time points after AngII infusion (n=10 for each time point). AngII indicates angiotensin II; BAPN, β-aminopropionitrile monofumarate; AAD, acute aortic dissection; CT, computed tomography; EVG, elastica Van Gieson; H&E, hematoxylin and eosin stain; and NE, norepinephrine.

Involvement of MMP9 in an AAD Model

When MMP9 expression levels were examined by reverse transcription polymerase chain reaction in the mouse aortic tissues 24 hours after the infusion of AngII, high levels were detected in the aortas from the BAPN/AngII-treated mice whereas aortas from the other groups showed weak or negligible expression (**Figure 4A**). Gelatin zymography showed gelatinolytic bands of 92 kDa and 87 kDa, which correspond to the latent and active forms of MMP9, respectively, but only in aortas from the BAPN/AngII-induced AAD mice, and not in aortas from the other groups (Figure 4B). Histological and immunohistochemical study showed that the accumulation of MMP9-positive cells, which also immunostained with antineutrophil antibody, localized to the media of the dissected aortas of BAPN/AngII-treated mice (Figure 4C). Film in situ zymography on the aortic tissues demonstrated that gelatinolytic activity was generated in the dissected area of the aortas from BAPN/AngII-treated mice, whereas the digestion was abrogated in gelatin film treated with 1,10-phenanthroline, and the nondissected aortas from control mice showed negligible activity (Figure 4D). These data indicate that metalloproteinases exist within the dissected aortic tissue. Although the experimental methods used were not specific to detect MMP9 activity, our findings including the zymographical data in the presence of an active MMP9 form suggest the possibility that pro-MMP9 derived from neutrophils infiltrated in the aortic media is activated within the tissue. To study the location of superoxide production within the aortic tissues, we used staining with dihydroethidium, which is specific for superoxide.[25] As shown in Figure 4D, strong fluorescence was detected in the dissected aortic tissue from the AAD mice, whereas control aortic tissue showed only a low-intensity fluorescence. More important, the infiltration of MMP9-positive neutrophils was demonstrated not only in the dissected media, but also in the intima of nondissected lesions of BAPN/AngII-induced AAD

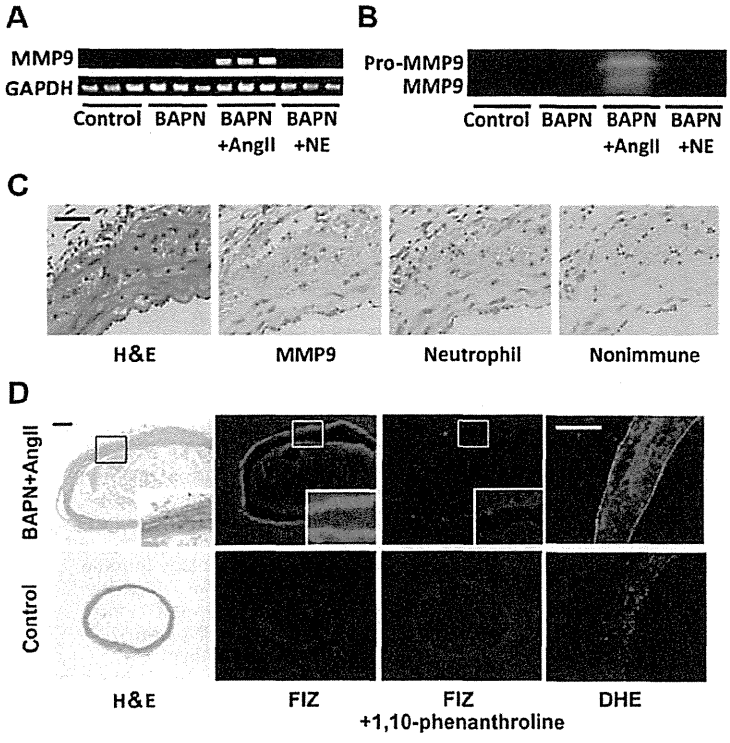

Figure 4. AAD in BAPN/AngII-treated wild type (WT) mice is accompanied by enhanced MMP9 expression, neutrophil infiltration, and superoxide production. **A**, Analysis of *MMP9* mRNA expression by reverse transcription polymerase chain reaction in aortic tissues from the WT mice treated with vehicle (control), BAPN, BAPN/AngII (BAPN+AngII), or BAPN/NE (BAPN+NE). Polymerase chain reaction products of 3 independent samples from each group are shown. **B**, Gelatinolytic activity of the aortic tissue homogenates was assessed by gelatin zymography. BAPN/AngII-treated WT aorta shows gelatinolytic bands of 92 kDa and 87 kDa, corresponding to pro-MMP9 and active MMP9, respectively. **C**, Serial paraffin sections of dissected thoracic aorta of BAPN/AngII-treated WT mice were stained with H&E and immunostained with anti-MMP9 antibody, antineutrophil antibody, or control immunoglobulin G. Note the infiltration of MMP9-positive neutrophils in the media of the dissected lesion. **D**, Film in situ zymography and dihydroethidium staining of aortic tissues from BAPN/AngII-treated or control vehicle-treated WT mice. Serial frozen sections were made and stained with H&E or subjected to film in situ zymography using gelatin films coated with or without 1,10-phenanthroline. Frozen sections were also stained with dihydroethidium. Scale bars, 200 μm. AAD indicates acute aortic dissection; BAPN, β-aminopropionitrile monofumarate; AngII, angiotensin II; WT, wild type; MMP9, matrix metalloproteinase 9; NE, norepinephrine; H&E, hematoxylin and eosin stain; FIZ, film in situ zymography; GAPDH, glyceraldehyde 3-phosphate dehydrogenase; and DHE, dihydroethidium.

thoracic aortas (Figure 5). In control mice treated with BAPN alone or BAPN and NE, immunostaining of MMP9 and neutrophils was only rarely observed in the tissues (Figure 5). These findings suggest that the increased levels of MMP9 detected in the AAD aortas are derived primarily from neutrophils that infiltrate both the aortic intima and media.

Reduction of AAD Incidence by Pharmaceutical and Genetic Depletion of MMP9 or by Neutrophil Depletion

To determine whether MMP9 plays a direct role in the AAD mouse model, BAPN/AngII-treated mice were treated with synthetic MMP inhibitor ONO-4817. As shown in Figure 6A, when ONO-4817 was administered orally on daily basis to BAPN-treated WT mice from 48 hours prior to AngII infusion until sacrifice, the incidence of AAD decreased significantly from 100% to 60%, and spontaneous death caused by aortic rupture was blocked completely. Consistent with these observations, when $MMP9^{-/-}$ mice were treated with BAPN/AngII, AAD incidence was attenuated remarkably to basal levels (10% of the $MMP9^{-/-}$ mice) whereas BAPN alone induced thoracic aneurysm formation at a frequency comparable with that observed in WT mice (Figure 6A and 6B). Hence, these findings support a direct role for MMP9 in the development of AAD.

Although multiple cell populations are capable of expressing MMP9 (eg, macrophages,[12] endothelial cells,[26] and vascular smooth muscle cells[24]), neutrophil infiltrates dominated the affected tissues. As such, we depleted neutrophils during aneurysm formation by treating the mice with anti-Gr-1

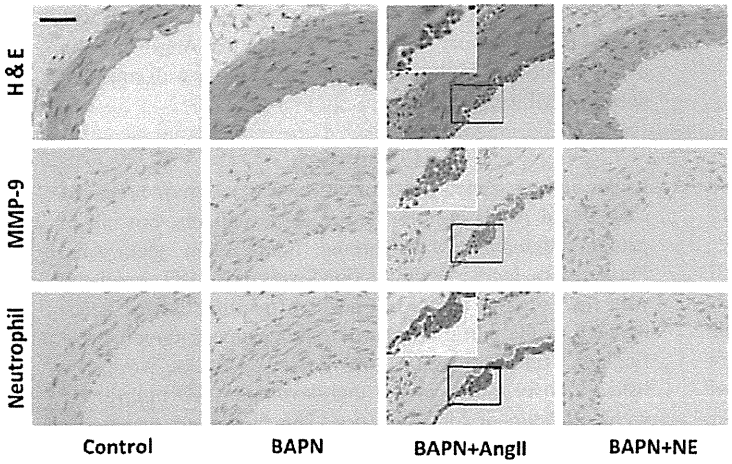

Figure 5. Infiltration of MMP9-positive neutrophils in the intima of nondissected lesions of BAPN/AngII-induced AAD thoracic aortas. MMP9 expression and neutrophil infiltration were examined by histology and immunohistochemistry in the aortas of untreated wild type mice (control) or wild type mice treated with BAPN alone, BAPN+AngII, and BAPN+NE. Note the accumulated MMP9-positive neutrophils in the intima of nondissected aorta from BAPN/AngII-treated mice. Inlets in the BAPN+AngII group show a higher-power view of the rectangular areas. Scale bar, 200 μm. MMP9 indicates matrix metalloproteinase 9; H&E, hematoxylin and eosin stain; BAPN, β-aminopropionitrile monofumarate; AngII, angiotensin II; AAD, acute aortic dissection; and NE, norepinephrine.

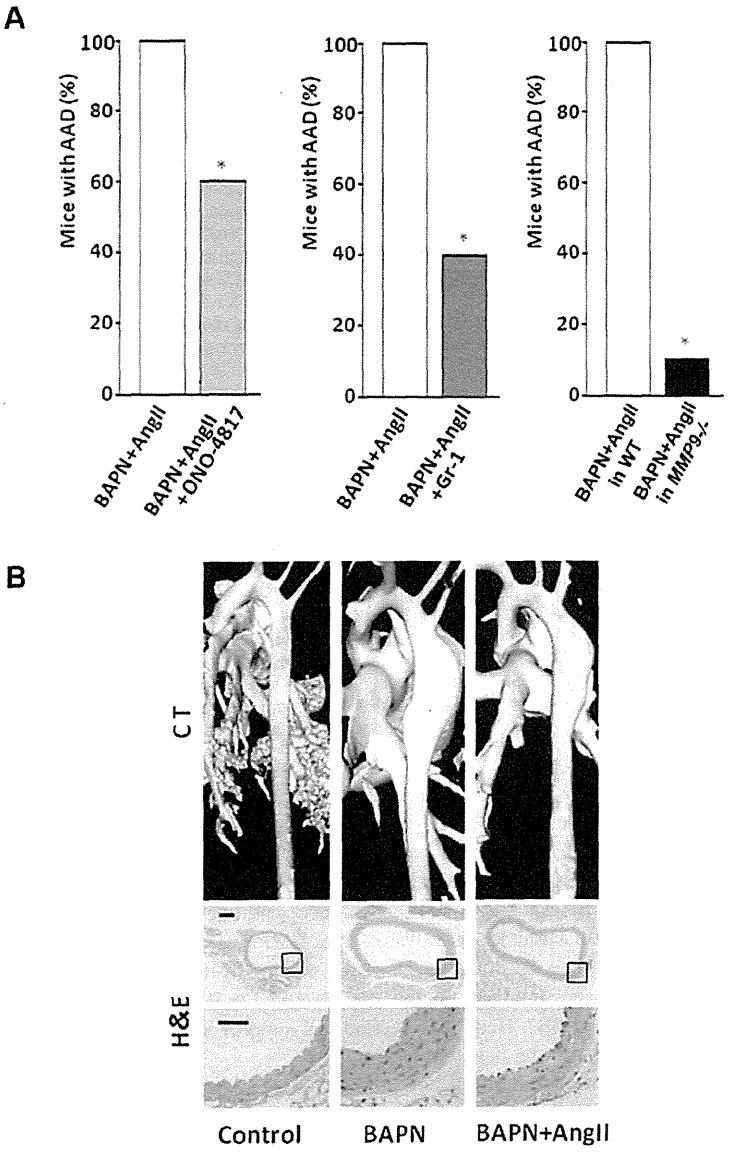

Figure 6. Pharmaceutical and genetic depletion of MMP9 or immunological depletion of neutrophils attenuates AAD incidence in mice. **A**, AAD incidence in BAPN/AngII-treated WT mice that were treated with ONO-4817 (BAPN+AngII+ONO-4817) (**left**) or anti-Gr-1 antibody (BAPN+AngII+Gr-1) (**middle**) and the incidence in BAPN/AngII-treated *MMP9*$^{-/-}$ mice (**right**) were compared with that in BAPN/AngII-treated WT mice (n=10 for each group). The probability value was adjusted with the Bonferroni method for pairwise comparisons. *$P<0.05$ versus BAPN/AngII-treated WT mice. **B**, Three-dimensional images of enhanced computed tomographic scan (**upper**) and histology (**middle** and **bottom**) of the aortas from *MMP9*$^{-/-}$ mice that were treated with vehicle for 4 weeks (control), BAPN alone for 4 weeks (BAPN), or BAPN for 4 weeks and then AngII for 24 hours (BAPN+AngII). Note that AAD formation is blocked in BAPN/AngII-treated *MMP9*$^{-/-}$ mice. (**Bottom**) High-power view of the rectangular areas in the middle panel. Scale bars, 200 μm and 100 μm for the middle and bottom panels, respectively. MMP9 indicates matrix metalloproteinase 9; AAD, acute aortic dissection; BAPN, β-aminopropionitrile monofumarate; AngII, angiotensin II; anti-Gr-1, anti-granulocyte-differentiation antigen-1; WT, wild type; and H&E, hematoxylin and eosin stain.

neutralizing antibody. The number of circulating neutrophils was reduced to 20% of control levels by intraperitoneal injection of the antibody for 48 hours prior to AngII infusion (data not shown), and, as expected, neutrophil depletion attenuated AAD incidence significantly (Figure 6A).

AngII-Induced Neutrophil Infiltration to Aortic Intima Independent From MMP9 Expression

Infiltration of neutrophils into the aortic intima was observed in BAPN/AngII-treated WT mice with or without ONO-4817 administration, as well as in BAPN/AngII-treated *MMP9*$^{-/-}$ mice (Figure 7A). Hence, these data demonstrate that AngII promotes neutrophil infiltration independent of MMP9 expression in our AAD model, but these results do not exclude the possibility that normal rates of neutrophil infiltration are maintained only within the noncross-linked, fragile vessel wall caused by chronic BAPN treatment. Thus, we further assessed the effect of AngII on neutrophil infiltration by infusing AngII in BAPN-untreated WT or *MMP9*$^{-/-}$ mice wherein vascular structural integrity is intact. As shown in Figure 7B, neutrophil infiltration into the aortic intima was unaffected between the 2 groups, indicating that AngII infusion evokes neutrophil infiltration to the intact aortic wall independent of MMP9 expression.

Discussion

In the current study, we demonstrated that serum levels of MMP9 and AngII are elevated in AAD patients, but not in patient populations with chronic, nonruptured aneurysms. Furthermore, increased circulating levels of MMP9 correlated with the presence of MMP9-positive neutrophils that accumulated in the aortic tissues of AAD patients. Given these findings from studies of human AAD specimens, we established a novel mouse model that develops AAD unfailingly within 24 hours of AngII infusion. This model was dependent on preconditioning mouse aortas with the lysyl oxidase

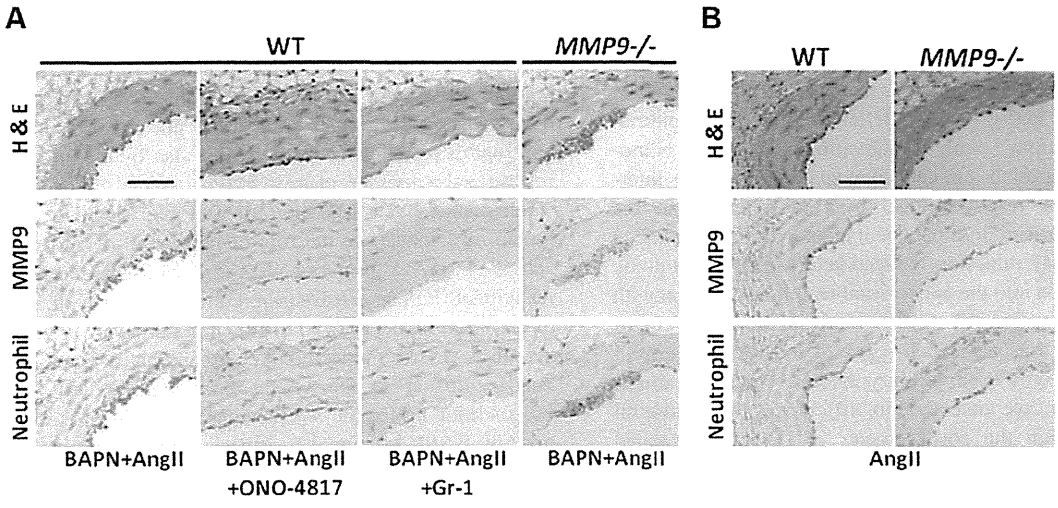

Figure 7. AngII-induced neutrophil infiltration in aortic intima is independent of MMP9 expression or BAPN treatment. **A**, Histological and immunohistochemical analyses of MMP9 expression and neutrophil infiltration in the aortic intima of the WT mice treated with BAPN and AngII (BAPN+AngII); BAPN, AngII, and ONO-4817 (BAPN+AngII+ONO-4817); or BAPN, AngII, and anti-Gr-1 antibody (BAPN+AngII+Gr-1); and those in the intima of the *MMP9*$^{-/-}$ mice treated with BAPN and AngII (BAPN+AngII) (n=10 for each group). Note that neutrophil infiltration is independent of MMP9 expression. Scale bar, 200 μm. **B**, Histological and immunohistochemical analyses of MMP9 expression and neutrophil infiltration in the aortic tissues of BAPN-untreated WT and *MMP9*$^{-/-}$ mice 24 hours after AngII infusion. Note that neutrophil infiltration is independent of BAPN treatment. Scale bar, 200 μm. AngII indicates angiotensin II; WT, wild type; MMP9, matrix metalloproteinase 9; H&E, hematoxylin and eosin stain; BAPN, β-aminopropionitrile monofumarate; and anti-Gr-1, anti-granulocyte-differentiation antigen-1.

inhibitor BAPN to create an aneurysmal, pre-AAD status in immature mice. Collagen and elastin cross-links, which are critical for maintaining vessel wall integrity, are disrupted by BAPN administration,[27] leading to the generation of mechanically fragile aortas that both display medial degeneration and develop aortic aneurysms. This type of aortic aneurysm is typically seen in human connective tissue diseases such as Marfan syndrome,[28] but the histology of cystic medial degeneration is commonly seen in aneurysms that arise secondary to aging and atherosclerosis as well.[3,4] It is not clearly elucidated whether aortic matrix cross-links are different between normal and aneurysmal aorta[29]; however, several studies from human pathological samples indicate that the composition of the aortic extracellular matrix changes as medial degeneration proceeds with enhanced deposition of proteoglycans and decreased collagen content, coupled with apoptosis of vascular smooth muscle cells.[30] These findings suggest that the aortic media and its matrix components are disorganized as a function of disease progression, thus leading to the generation of an aneurysmal aorta with weakened mechanical properties. As such, our mouse model would appear to recapitulate a similar state in which suitable triggers, such as AngII, precipitate the transition from a preconditioned, chronic aortic aneurysm to AAD.

Previous studies have suggested possible roles for MMP9 in the development of chronic atherosclerosis-derived aneurysms as well as connective tissue disease-related aortic aneurysm.[31–33] By contrast, our findings demonstrate that AAD formation itself proceeds in an MMP9-dependent fashion that is inhibited significantly by either pharmacological or genetic targeting of MMP9. A previous study by Gough et al[12] has shown that macrophages overexpressing autoactivating MMP9 induce atherosclerotic plaque rupture by disruptions of fibrous cap in apolipoprotein E mice, suggesting the ability of MMP9 to destroy aortic tissue. Altogether, these data support the notion that MMP9 is responsible for triggering aortic dissection from the preconditioned aneurysmal aorta. We have further demonstrated that neutrophil infiltration is observed in the intima of the predissecting aorta as well as in the dissected media, and that neutrophil depletion attenuates AAD incidence significantly. The importance of inflammation in the pathogenesis of vascular diseases is well documented, but until now, it has been difficult to determine whether neutrophil accumulation triggers dissection or occurs as a consequence of the massive vascular damage that develops during dissection. Because MMP9-positive neutrophils were confined to the intima of nondissected lesions while the dissected lesions displayed strong staining for MMP9-positive neutrophils primarily within the media, we posit that neutrophils infiltrate the intima at the initiation of dissection. Despite the importance of neutrophils, we cannot rule out the contribution of other immune effector cells that might be recruited subsequent to the inflammatory responses initiated by infiltrating neutrophils, as depleting neutrophils attenuated AAD, but not to the degree observed with *MMP9* targeting. Indeed, the upregulated *MMP9* mRNA levels detected in AAD aortic samples 24 hours after AngII infusion could result from nonneutrophil effector cells, because neutrophil MMP9 synthesis is mostly completed at earlier stages of differentiation, with mature neutrophils primarily storing MMP9 in granule compartments.[34] Nevertheless, the rapid induction of aortic dissection in our model as early as 6 hours after AngII infusion, in tandem with the accumulation of MMP9-positive neutrophils, supports the conclusion that infiltrating neutrophils trigger the initiation of dissection directly or indirectly.

MMP9 is a multifunctional proteinase endowed with the ability to degrade multiple extracellular matrix macromolecules, including types III, IV, and V collagens; denatured